New approaches to the imaging of surface potentials

2001 J. Phys.: Condens. Matter 13 10665

(http://iopscience.iop.org/0953-8984/13/47/309)

INSTITUTE OF PHYSICS PUBLISHING JOURNAL OF PHYSICS: CONDENSED MATTER

J. Phys.: Condens. Matter **13** (2001) 10665–10675 PII: S0953-8984(01)26964-1

New approaches to the imaging of surface potentials

U Weierstall, G G Hembree and J C H Spence

Department of Physics, Arizona State University, Tempe, AZ 85287, USA

E-mail: weier@asu.edu and spence@asu.edu

Received 19 July 2001, in final form 10 September 2001
Published 9 November 2001
Online at stacks.iop.org/JPhysCM/13/10665

Abstract

Towards the goal of recording and analysing the elastically filtered intensity of 4–50 keV electrons within the two-dimensional reflection rocking curves (convergent-beam RHEED patterns), preliminary experiments with a one-dimensional serial energy filter have been performed. Zero-loss and plasmon-loss filtered linescans through the specular disc of a CB-RHEED pattern from the Si(001)-2×1 surface at 4 kV are shown and compared with dynamical calculations. Energy-filtered detection of CB-RHEED patterns is necessary for quantitative analysis of the surface potential.

1. Introduction

The recent dramatic improvements with which multiply scattered high-energy transmission electron diffraction (HEED) data can be quantified has not yet been matched by corresponding improvements at lower energies in surface science. These improvements in HEED have resulted from the availability of energy filters and from the use of sufficiently small and intense probes which ensure crystalline perfection within the region studied. As one example among several, see [1], in which an accuracy of better than 1% in low-order structure measurement by HEED has allowed the 'imaging' of the bonding charge-density in oxides.

No fundamental reason should prevent similar quantitative advances in LEED and RHEED; however, the task is simpler for several reasons when using convergent-beam RHEED at higher energies. If similar accuracy could be achieved in the measurement of the surface potential by comparison of multiple-scattering calculations with model potentials, similar charge-density maps might be obtained for surfaces. These would deepen our understanding of surface chemistry and the reactions which occur during adsorption.

Towards this goal, we have constructed a convergent-beam RHEED apparatus with energy filtering [2] and developed appropriate multiple-scattering software simulation techniques [3]. The advantages of the CB-RHEED geometry for this work are: (i) as for HEED, accurate quantification requires the study of defect-free regions and the focused probe in CB-RHEED allows single-domain patterns to be obtained; (ii) the theoretical complexities of very low energies (e.g. in LEED) can be avoided. In particular, the exchange-correlation corrections

between beam and crystal electrons are small at energies above a few kilovolts, again as in HEED. These corrections must be less than the modifications to surface charge-density sought. (iii) The large illumination angle provides additional information, since a complete rocking curve can be recorded in every diffracted order simultaneously. (iv) By focusing the probe just before the sample, a shadow image may be formed within the divergent specular beam. At high resolution, this may be interpreted as a Gabor in-line hologram. Experimental results from this reflection holography technique can be found in [4], where a field-emission nanotip is used to provide the diverging beam in a lensless geometry. Practical advantages of the RHEED geometry also include the space allowed above the sample, the extreme sensitivity of electron scattering compared to other probes, and the possibilities which the strong scattering provides for time-resolved studies of chemical reactions.

In previous work, CB-RHEED patterns have been obtained using TEM or STEM instruments, often resulting in a compromise in vacuum conditions. For a review of surface imaging by reflection (REM) in the UHV TEM (including the formation of elastically filtered images), see [5]. The STEM instrument (operating in the reflection mode with perhaps 100 kV electrons), however, offers the advantages of the smallest sub-nanometre probes (obtained from a field-emission source): a sub-nanometre imaging capability (if the probe is scanned) and limited energy-filtering capabilities [6]. All CB-RHEED experiments reported so far have been done in high vacuum conditions (10^{-6}–10^{-7} Torr in TEM without energy filter [7–9] and with energy filter [10] and 10^{-5} Torr in a specially built diffraction camera [11, 12]). Since RHEED is extremely surface-sensitive, contamination significantly affects the diffraction pattern and limits the possible surfaces that can be studied in conventional TEM. Impressive results have also been obtained from dedicated UHV RHEED systems which do offer energy filtering, but which lack a focused probe [9–11, 13–15]. Our aim, then, is to record and analyse the elastically filtered intensity of 4–50 keV electrons within the two-dimensional reflection rocking curve. The sensitivity of the specular disc, for example, has been studied in detail [16]. We treat crystal surfaces of known structure in order to map out the surface potential, particularly in the direction normal to the surface, which controls the docking of approaching molecules at intermediate and large distances where quantum forces can be neglected.

2. Instrumentation

Figure 1 shows a schematic diagram of our instrument. The optic axis is vertical and two bakeable magnetic lenses are used in combination with an LaB_6 source to produce an electron probe of about 1 μm diameter. The highest energy obtainable from the Kimball Physics electron gun is 50 keV. The working distance is 50 mm and the apertures and beam current controls allow variation of the beam convergence. Collimated illumination, producing a conventional RHEED pattern, is obtained by focusing the beam on the detector screen rather than on the sample. A double-tilt heating stage has been designed, which rotates into the transmission geometry. Residual gas pressure during observation is 3×10^{-10} Torr.

The viewing system consists of a transmission phosphor screen made on an ITO coated glass disc. This screen is imaged through a 4 inch diameter UHV window by a 1024×1024 optically coupled liquid-nitrogen-cooled CCD camera, by use of a diagonal front-surface mirror.

We have evaluated the use of a retarding potential mesh filter to obtain quasi-elastic CB-RHEED patterns [2, 17]. Although energy loss spectra and filtered CB-RHEED discs were successfully obtained, we have since found this system inadequate, in view of the distortion of the CB-RHEED pattern produced by the mesh. We have therefore replaced this mesh filter

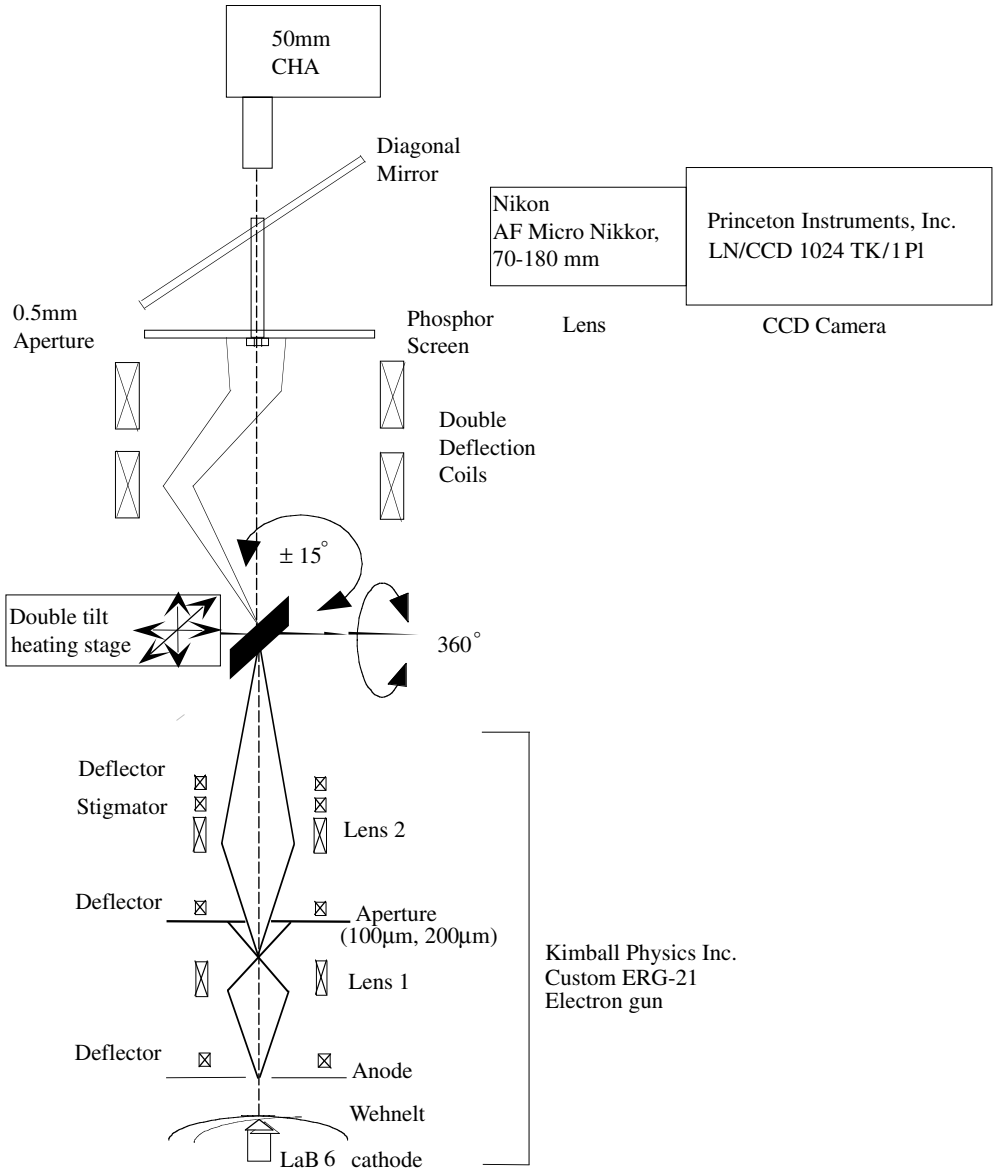

Figure 1. Schematic view of the CB-RHEED diffraction camera. CHA: concentric hemispherical energy analyser.

with a scanned aperture filter, as shown in figure 1. This new filter was constructed using a design similar to the detector section of the instrument built by Meyer-Ehmsen and co-workers [15]. A set of magnetic double-rocking deflection coils following the sample is used to scan the CB disc over a 0.5 mm diameter aperture, giving an angular resolution of 0.8 mrad. The aperture is placed in a hole in the centre of the phosphor screen. The electrons selected by the aperture pass through a flight tube and into the input lens of a 50 mm concentric hemispherical energy analyser (CHA). This analyser can achieve an energy resolution of 1 eV at 5 keV electron kinetic energy. In the work reported here we have chosen a resolution of

1.6 eV as a compromise between collected intensity and resolution. To prevent high voltage discharge in the analyser, the experiments were performed at 4 keV electron energy.

Data collection was accomplished with a National Instruments PC card programmed in LabView. TTL pulses from the CHA charge-sensitive amplifier were counted in step with the voltage used to program the deflection of the CB-RHEED disc across the aperture. Line scans through the discs were programmed along the specular scattering direction and averaged 20 times to reduce the influence of electron intensity fluctuations and achieve reasonable counting statistics. Acquisition of a single line scan (with averaging over 20 scans) took 1 hour. For this reason alone parallel energy filtering of a whole disc would be superior to the serial filtering carried out here. This possibility will be discussed further in the conclusion.

3. Experiments

The experiment was done using a Si(001) (0.02 Ω cm, n-doped, misorientation $<0.5^\circ$) wafer. The sample was outgassed overnight at 400 °C and then flash-heated to 1200 °C for 10 s. This treatment produces mixed surface structures of 2×1 and 1×2 domains [18]. Subsequently the sample was annealed for 20 min at 1000 °C to obtain a single domain Si(001)-2×1 structure [19]. As shown previously [3] a CBED pattern from a single 2×1 domain with the beam centred at the [110] azimuth contains superstructure discs in the zero-order Laue zone and no half-order Laue zone. A single 1×2 domain produces a pattern with no superstructure discs in the zero-order Laue zone and superstructure discs in the half-order Laue zone.

Figure 2(a) shows a convergent-beam RHEED pattern obtained with our system at 12 kV from the silicon (001)-2×1 surface without energy filtering. Due to the diffraction geometry and unlike the transmission case, the envelopes of the convergent beam discs are distorted for non-specular discs. The electron beam was centred at the [110] azimuth and the angle of incidence was about 3.6°. The probe position on the sample was aligned to maximize the intensity in the superstructure discs $\left(\frac{1}{2}0\right)$ and $\left(\frac{\bar{1}}{2}0\right)$ in the zero-order Laue zone, i.e. the probe position is on a single 2×1 domain. Only the zero-order Laue zone is shown. The complex pattern visible in the diffracted discs is highly sensitive to the surface structure as shown previously [3]. The pattern for the same diffraction conditions at 4 kV exhibits less fine structure and the disc edges are not as sharp (figure 2(b)). Possible reasons are the increased inelastic scattering at lower energy, increased probe size and AC stray field effects.

To compare this CB-pattern with simulations, multiple scattering calculations based on an experimental structure model derived from x-ray diffraction results [20] have been made. This model has a dimer tilt angle of 7.8°. A comparison of this structural model with a different model determined from LEED data [21] has shown better agreement of our experimental data with the x-ray model [3]. In the calculations the Schrödinger equation is solved for a crystal slab of finite thickness, which is divided into a surface and bulk layers. The slab is cut into slices parallel to the surface and the electron propagation within each slice is calculated using the *R*-matrix method suggested by Zhao *et al* [22]. Details of the calculations are given elsewhere [3].

Figure 2(c) shows the calculated pattern at 4 kV for the Si(001)-2×1 single domain surface with the beam centred at the [110] azimuth and 90 mrad incidence angle at the centre of the specular disc. In this calculation the incident beam was perpendicular to the dimerization direction, i.e. superstructure discs in the zero-order Laue zone are visible. The calculation includes 15 beams in the zero-order Laue zone for diagonalization. Evanescent waves are included using Bethe potentials [23]. The experimental pattern has a mirror symmetry, which indicates that the average dimer configuration is symmetrical within the illuminated area

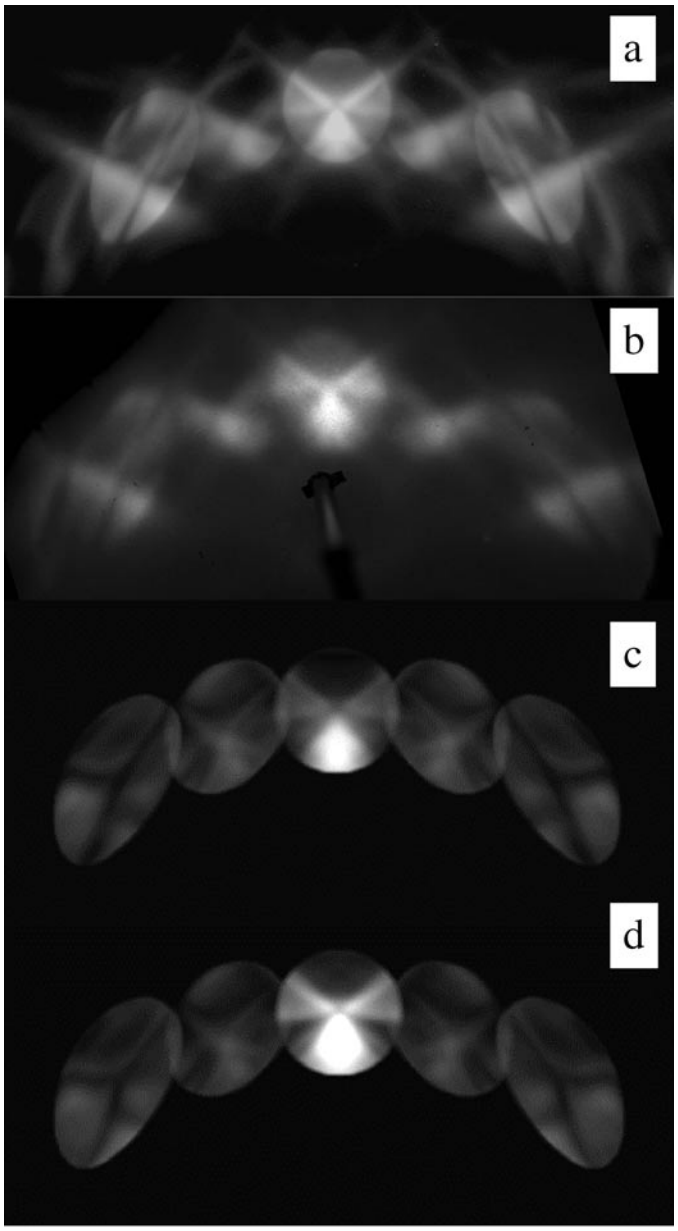

Figure 2. (a) CB-RHEED pattern at 12 kV from the silicon (001)-2 × 1 surface without energy filtering. Due to the diffraction geometry in RHEED the envelopes of the convergent beam discs are distorted for non-specular discs. The electron beam is centred at the [110] azimuth and the incidence angle is about 3.6°. (b) The pattern for the same diffraction conditions at 4 kV exhibits less fine structure and the disc edges are not as sharp. Energy-filtered linescans were obtained through the centre of the specular disc. (c) Calculated pattern at 4 kV for the Si(001)-2 × 1 single domain surface with the beam centred at the [110] azimuth and 90 mrad incidence angle at the centre of the specular disc. Incident beam perpendicular to the dimerization direction, i.e. superstructure discs $\left(\frac{1}{2}0\right)$ and $\left(\bar{\frac{1}{2}}0\right)$ in the zero-order Laue zone are visible. (d) Averaged pattern for both dimerization directions (two-domain pattern). The intensities in the specular disc agree better with the experiment in (b).

(i.e. there is no preferred dimer tilt in one direction). This symmetry could result from averaging over areas with opposite dimer tilts (see also [3] for more possible reasons for symmetry) due to the relatively large probe size of 1 μm. Since the calculation uses a supercell with only one dimer tilt and therefore gives an asymmetric pattern, we averaged two CB-RHEED patterns with opposite dimer tilts to simulate incoherent superposition. The discs overlap slightly as in the experiment and there is reasonable qualitative agreement in the patterns between experiment and calculation. Nevertheless, it is apparent that the relative intensities in the calculated specular disc are different from the experiment. Assuming that the surface within the illuminated area is not a perfect single-domain structure, but a mixture of two domains, we calculated the CB-RHEED pattern for the other domain (incident beam parallel to dimerization direction) and averaged it with the previous pattern, assuming incoherent superposition. This is shown in figure 2(d). Now the relative intensities in the specular disc agree more with the experiment. Linescans through the specular disc can further clarify this point.

Figure 3(a) shows a linescan through the centre of the specular disc of the 4 kV CB-RHEED pattern, which represents a rocking curve containing both elastically and inelastically scattered electrons. A zero-loss energy-filtered linescan through the same area of the specular disc recorded with the CHA is shown in figure 3(b). The linescan contains 75 points, each recorded with a dwell time of 5 s. Typical count rates were 5 counts/s. The shape of the elastically filtered linescan is very similar to the unfiltered rocking curve. Outside the disc the intensity is zero for the filtered linescan whereas in the unfiltered pattern there is a diffuse background between the Bragg discs (visible in figure 2(b)). Inelastic processes contributing to the background are phonon scattering, plasmon scattering and single-electron excitations [24]. Phonon scattering involves large scattering angles but very small energy losses (about 30 mV). These are not excluded by zero-loss filtering. Plasmon losses involve larger energy losses (about 12–20 eV) and small scattering angles. Since the background between the Bragg discs is almost entirely removed by zero-loss filtering, which has also been shown with a mesh filter [2, 17], this background must be due to coupled phonon–plasmon scattering as in HEED [25].

Figure 3(c) shows two calculated elastic rocking curves through the centre of the specular disc for the Si(001)-2 $\times$ 1 surface at the [110] azimuth and 90 mrad incidence angle at the centre of the specular disc (4 keV electron energy). One curve is calculated for a single domain surface (linescan through the specular disc of figure 2(c)) the other is an average over rocking curves from two different domains (linescan through the specular disc of figure 2(d)). Comparison with the zero-loss filtered and the unfiltered rocking curve shows that the position of the maximum of the experimental curves agrees only with the two-domain calculation. Therefore it is likely that the surface within the illuminated area is not a perfect single domain area, which can be attributed to an increased probe size of more than 1 μm at 4 keV or imperfect surface preparation. The agreement of the shape of the experimental and calculated curves is not perfect, which is still a common problem in RHEED calculations.

The ratio of the intensity at the maximum of the rocking curve to the intensity of the incident beam gives a reflectivity of 0.007 for the zero-loss-filtered signal and 0.02 for the unfiltered signal at this incidence. Therefore, only about 27% of the total reflected intensity is due to elastic (including phonon-scattered) electrons at this incidence angle (88 mrad). This percentage decreases with smaller incidence angle. The reflectivity is much lower than the calculated elastic reflectivity. The reason could be that the surface within the illuminated area is not perfect and part of it does not contribute to the reflected signal or the surface is disordered which leads to diffuse scattering. A smaller probe size is therefore highly desirable. The calculated intensities depend strongly on the imaginary potential used to treat surface plasmon

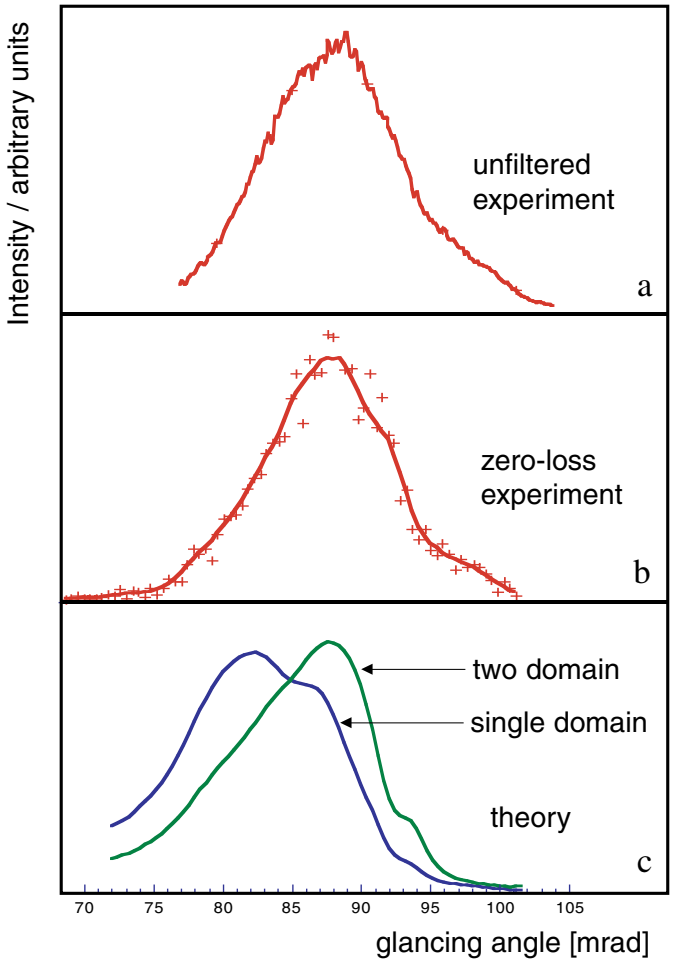

Figure 3. (a) Linescan through the centre of the specular disc of the 4 keV CB-RHEED pattern in figure 2(b). (b) Zero-loss energy-filtered linescan through the same area of the specular disc as in (a). (c) Calculated elastic rocking curves through the centre of the specular disc for the Si(001)-2 × 1 surface at the [110] azimuth and 90 mrad incidence angle at the centre of the specular disc (4 kV electron energy). Curve 'single domain' is calculated for a single domain surface (corresponding to figure 2(c)), 'two-domain' is an average over rocking curves from two different domains (corresponding to figure 2(d)). The location of the maxima of the experimental curve agrees with the two-domain calculation.

losses [26, 27]. We use in this calculation an empirical mean absorption potential of the form [28]

$$V_0'(z) = \begin{cases} V_0' \exp\left(-a(z - z_0)^2\right) & z > z_0 \\ V_0' & z < z_0 \end{cases}$$

The amplitude V_0' and damping a are treated as parameters which are adjusted to obtain agreement between experimental and calculated CB-RHEED patterns, z_0 is the position of the top surface atomic layer. The values used here are $V_0' = 1, a = 0.5$. It has recently been observed experimentally that elastic filtering changes the relative intensities of rocking curves and that incorporation of an extended absorption potential into calculations to account for

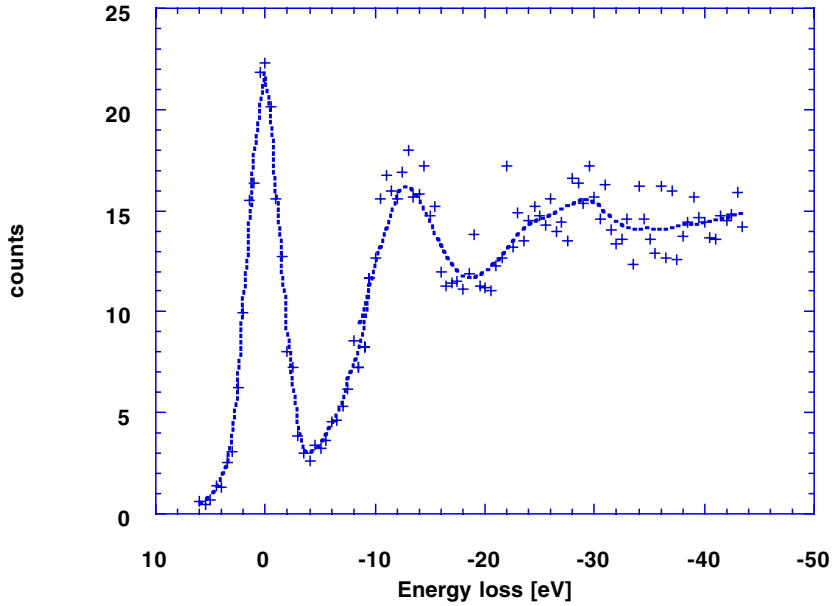

Figure 4. Energy spectrum from the centre of the specular disc (figure 2(b)) diffracted off the Si(100) surface at 4 keV kinetic energy. The curve was fitted with a locally weighted least squares error method. The measured full width at half maximum of the zero-loss peak is 3.3 eV. The surface plasmon peak at 11.3 eV is resolved.

plasmon losses can lead to shifts in rocking curve maxima [27]. Therefore, further study of the surface plasmon influence on the elastic rocking curve is necessary for quantitative analysis of RHEED intensities. This is different to the situation in HEED where plasmon scattering contributes to the mean absorption only [25] and therefore elastic filtering does not change relative intensities but dramatically reduces the background and changes absolute intensities.

If the CHA energy is scanned while the collected angle is kept fixed an energy spectrum of the scattered electrons can be obtained. Figure 4 shows such a spectrum from the centre of the specular disc (figure 2(b)) diffracted off the Si(100) surface at 4 keV kinetic energy. The measured full width at half maximum of the zero loss peak is 3.3 eV. This value is larger than expected from a LaB_6 source: 1.8 eV. AC magnetic fields may be broadening the observed energy spread. The surface plasmon peak at around 11.3 eV is resolved.

Figure 5 shows a comparison of two rocking curves obtained by the filter pass energy set at the elastic peak and at the surface plasmon peak. Both rocking curves look very similar which is in agreement with observations in HEED [29] where plasmon-loss-filtered Bragg discs look similar to elastic Bragg discs except that they are blurred.

Our linescans through CB-RHEED discs cover only a small range of glancing angles compared to rocking curves recorded with conventional RHEED instruments. But this limited range is compensated by the higher information content of the two-dimensional CB-RHEED pattern compared to the conventional one-dimensional rocking curve. The changes in relative intensities after elastic filtering observed in [27] occur in the direction of the reciprocal rods normal to the surface and seem to be only appreciable when the intensity is recorded along a large portion of the rod. Since our findings so far show no significant change of the shape of elastic linescans through CB-RHEED discs compared to the unfiltered scans and because of the high sensitivity of the CB patterns to changes in the surface structure, it may be possible

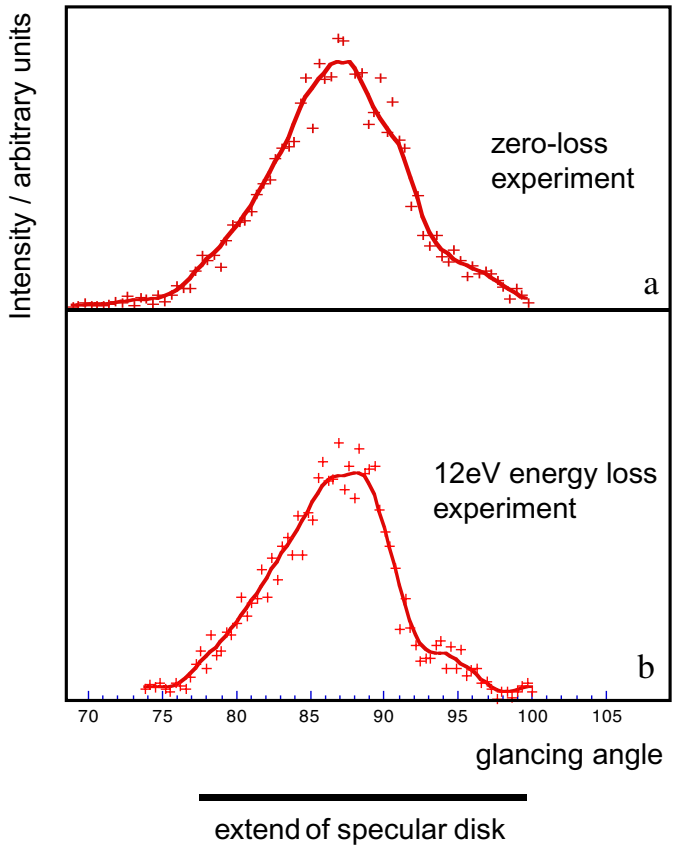

Figure 5. Comparison of two linescans through the specular disc in figure 2(b) obtained with the filter pass energy set at the elastic peak and at the surface plasmon peak. (a) Zero-loss filtered, (b) surface plasmon-loss filtered (pass energy set at 12 eV).

to refine atomic positions from CB-RHEED patterns based on pattern matching only, without energy filtering. There have been several successful attempts at surface structure refinement from elastic and unfiltered rocking curves with an automated fitting procedure [30–32], but the agreement between the calculated and experimental rocking curves does not yet match the accuracy achieved in HEED.

For a quantitative analysis of the surface potential and its bonds, energy filtering will be necessary. An imaging filter as used in HEED would better exploit the advantage of parallel detection in convergent beam electron diffraction. Intensity fluctuations of the electron gun, which are a problem with serial detection and with conventional RHEED, would not be a problem. Recording a whole disc with our serial filter would require an excessive amount of time. RHEED intensity variations inside the diffracted disc (double rocking) provide a more stringent test of theory than in conventional RHEED (especially symmetry information is more easily recognized than in one-dimensional linescans). A filter with a large acceptance angle and low aberrations is required, since the divergence angle of the incident beam is typically about 0.5° (half angle) for non-overlapping discs from Si(001). It would be enough to filter one disc at a time, thus reducing the necessary angular range used in the filter. Higher kinetic energy of 12 keV improves the quality of the patterns as shown in figure 2(a). We cannot use

higher energies with our serial filter due to high voltage instabilities. The relevant imaging filter would be an omega-filter as used in several TEMs, an alpha-filter [33] or an imaging Wien-filter [34, 35] which has the advantage of a straight optic axis, but needs a retarding and accelerating lens before and after the filter, respectively, to achieve high energy resolution.

4. Conclusions

To explore the possibility of measuring elastic two-dimensional rocking curves from CB-RHEED patterns for quantitative analysis, a concentric hemispherical energy analyser has been added to our UHV diffraction camera. Energy-filtered linescans through CB-RHEED patterns have been obtained at 4 kV. The energy resolution is 1.6 eV and the angular resolution is 0.8 mrad. The preliminary results show that the elastic filtered linescans through the specular disc have a similar shape to the unfiltered linescans for the small range of glancing angles measured. The plasmon-loss rocking curve through the specular disc has also similar shape to the elastic rocking curve in analogy to HEED. Measured rocking curves from Si(001) at 4 kV agree better with calculations for a two-domain surface than a single domain surface. For quantitative analysis of the surface potential and surface bond-charge distributions, energy filtering will be necessary. For an *ab initio* calculation of the surface potential see [36]. An imaging energy filter is necessary to take advantage of the much higher information content present in a two-dimensional CB-RHEED pattern compared to a one-dimensional rocking curve. Modelling of the imaginary part of the optical potential used to represent the effects of inelastic (e.g. plasmon) scattering on elastic scattering is more complex than in the transmission case, but may be parametrized in a similar way.

Acknowledgments

This work was supported by NSF award DMR9814055.

References

[1] Zuo J M, Kim M, O'Keeffe M and Spence J C H 1999 *Nature* **401** 49
[2] Weierstall U, Zuo J M, Kjorsvik T and Spence J C H 1999 *Surf. Sci.* **442** 239
[3] Zuo J M, Weierstall U, Peng L M and Spence J C H 2000 *Ultramicroscopy* **81** 235
[4] Spence J C H, Zhang X, Weierstall U, Zuo JM, Munro E and Rouse J 1997 *Surf. Rev. Lett.* **4** 577
[5] Spence J C H 1995 *Energy Filtered Electron Microscopy* ed L Reimer (New York: Springer)
[6] Cowley J M 1989 *Ultramicroscopy* **27** 319
[7] Shannon M D, Eades J A, Meichle M E, Turner P S and Buxton B F 1984 *Phys. Rev. Lett.* **53** 2125
[8] Peng L M and Cowley J M 1987 *J. Electron Microsc. Tech.* **6** 43
[9] Smith A E and Lynch D F 1988 *Acta Crystallogr.* A **44** 780
[10] Lordi S, Ma Y and Eades J A 1994 *Ultramicroscopy* **55** 284
[11] Ichimiya A, Kambe K and Lehmpfuhl G 1980 *J. Phys. Soc. Japan* **49** 684
[12] Lehmpfuhl G and Dowell W C T 1986 *Acta Crystallogr.* A **42** 569
[13] Muller B and Henzler M 1997 *Surf. Sci.* **389** 338
[14] Horio Y 1996 *Jap. J. Appl. Phys.* **35** 3559
[15] Britze K and Meyerehmsen G 1978 *Surf. Sci.* **77** 131
[16] Ichimiya A 1987 *Surf. Sci.* **192** L898
[17] Horio Y, Hashimoto Y and Ichimiya A 1996 *Appl. Surf. Sci.* **101** 292
[18] Doi T and Ichikawa M 1989 *J. Cryst. Growth* **95** 468
[19] Sakamoto T and Hashiguchi G 1986 *Jap. J. Appl. Phys.* **25** L78
[20] Jedrecy N, Sauvagesimkin M, Pinchaux R, Massies J, Greiser N and Etgens V H 1990 *Surf. Sci.* **230** 197
[21] Over H, Wasserfall J, Ranke W, Ambiatello C, Sawitzki R, Wolf D and Moritz W 1997 *Phys. Rev.* B **55** 4731
[22] Zhao T C, Poon H C and Tong S Y 1988 *Phys. Rev.* B **38** 1172

[23] Peng L M, Dudarev S L and Whelan M J 1996 *Surf. Sci.* **351** L245
[24] Egerton R F 1996 *Electron Energy-Loss Spectroscopy in the Electron Microscope* 2nd edn (New York: Plenum)
[25] Spence J C H and Zuo J M 1992 *Electron Microdiffraction* (New York: Plenum)
[26] Horio Y 1997 *Surf. Rev. Lett.* **4** 977
[27] Hara S, Watanabe K, Horio Y and Hashimoto I 1999 *Phys. Status Solidi* a **176** 925
[28] Jones R O and Jennings P J 1988 *Surf. Sci. Rep.* **9** 165
[29] Xu P R, Loane R F and Silcox J 1991 *Ultramicroscopy* **38** 127
[30] Witte M and Meyerehmsen G 1995 *Surf. Sci.* **326** L449
[31] Stock M and Meyerehmsen G 1990 *Surf. Sci.* **226** L59
[32] McCoy J M, Korte U and Maksym P A 1998 *Surf. Sci.* **418** 273
[33] Lanio S 1986 *Optik* **73** 99
[34] Tsuno K 1993 *Rev. Sci. Instrum.* **64** 659
[35] Rose H 1987 *Optik* **77** 26
[36] Kim M Y, Zuo J M and Spence J C H 1998 *Phys. Status Solidi* a **166** 445